EUROPEAN ORGANIZATION FOR NUCLEAR RESEARCH

CERN/SPSC 2002–034
SPSC/P284 Add. 3
28 October 2002

DIRAC BEAM REQUEST IN 2003

DIRAC Collaboration

GENEVA
2002

Contents

1 Introduction

This document is motivated by the need of DIRAC for additional beam-time in order to study and reduce systematic errors. In the recent recommendation CERN/DG/Research Board 2002-341, DIRAC was asked to provide clarifications to the SPSC on its beam-time request for the year 2003.

We recall that the goal of DIRAC is to determine the difference between the $I = 0$ and $I = 2$ S-wave $\pi\pi$ scattering lengths, $\Delta = |a_0 - a_2|$, from a measurement of the lifetime of $\pi^+\pi^-$ atoms ($A_{2\pi}$). The original goal of the experiment was to determine Δ with an accuracy of 5%.

After commissioning of the apparatus in fall 1998, the data collected in 1999 was essentially dedicated to the tuning and calibration of the detector and its read-out and DAQ, and the detection of $A_{2\pi}$ with the platinum target. The DIRAC experiment has then been collecting physics data, from 2000 to 2002. In total, 17.5 months of beam-time were allocated for physics studies, of which 12% were lost due to unforeseen problems in the PS accelerator complex. Based on these data we should reach a statistical accuracy on the lifetime is of the order of 14% (which translates into 7% uncertainty on $|a_0 - a_2|$).

In the course of detailed analysis it turned out, that a number of factors may lead to systematic errors. The assessment of these systematic errors requires special measurements, which the collaboration considers mandatory for a scientifically sound result. To accomplish this task additional beam-time in 2003 is required.

Hereafter, we outline the possible sources of systematic uncertainties and propose experimental means to measure them.

2 Reconstruction procedure

The experimental set-up is shown in Fig. 1

Let us shortly describe our reconstruction procedure to give the main idea about sources of systematic errors.

The event selection from the raw data is based on unambiguous reconstructability of a track pair originating from the target. The reconstruction efficiency is of the order of 55%.

The procedure is as follows:

- first, tracks in each arm is reconstructed as a straight line from the DC and VH informations.
- each track is transferred through the magnet and continued as a straight line to the target. This provides a first estimate of the momentum.
- The SFD are checked for hits close to the intersection of the above tracks with the SFD planes.
- The associated SFD hit (horizontal coordinate) is used for a new determination of the momentum.

The procedure looks straight forward, but there are various aspects and features which may lead to false reconstruction:

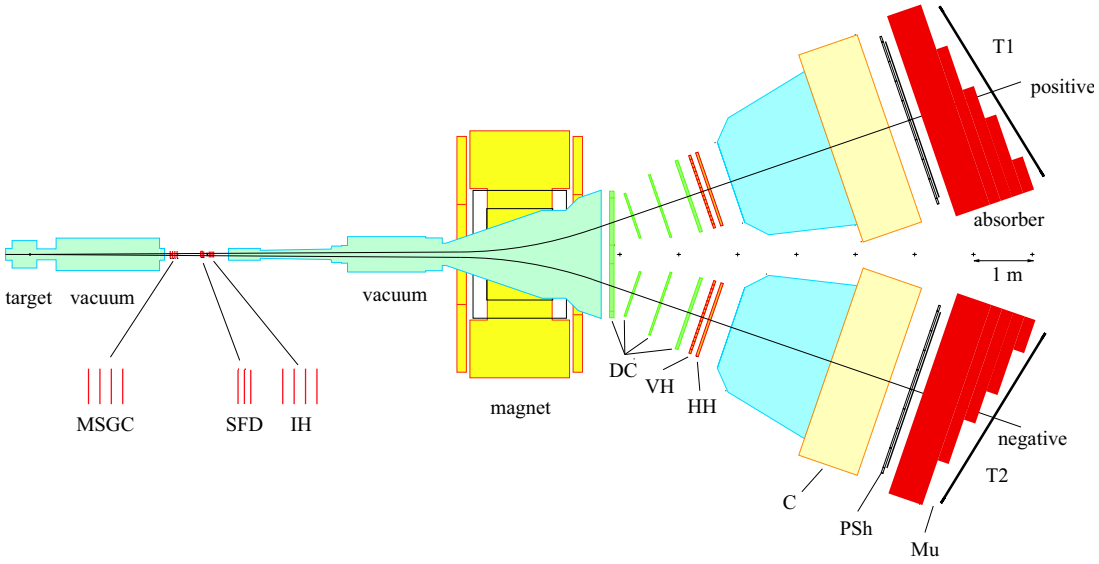

Figure 1: *Schematic top view of the DIRAC spectrometer. MSGC – microstrip gas chambers, SFD – scintillating fibre detectors, IH – ionization hodoscopes, DC – drift chambers, VH,HH – vertical and horizontal hodoscopes, C – Cherenkov counters, PSh – preshower detectors, Mu – muon detectors.*

- due to multiple scattering the upstream coordinate detectors altogether produce a kink in the track which leads to a sagitta as large as 1 cm. For small Q (close lying hits) the track-hit assignment may become ambiguous.
- due to multiple scattering in the downstream detectors and especially in the aluminium membrane at the exit of the vacuum chamber, the downstream tracks may already provide wrong inclinations and thus wrong momenta or wrong hit expectations in the SFD.
- the SFD detector suffers from a small optical leakage to adjacent fibers. In order to suppress more than one hit per track, a signal processor is used, which merges simultaneous (prompt) signals from adjacent fibers into one signal. However, this leads also to merging of two adjacent real hits from two close lying tracks and to an additional uncertainty in SFD coordinates. The merging is inactive for time-wise separated events (accidentals).
- any loss of one hit in the SFD due to inefficiency may produce a candidate for a presumed merged hit from two tracks.

All these features may lead to systematic errors. In the following sections the uncertainties which can be measured or significantly reduced due to dedicated measurements are discussed.

3 Signal extraction and sources of systematic errors

The experimental method proposed for the $A_{2\pi}$ lifetime measurement relies on the correct description of the time-correlated background from free (Coulomb and non-Coulomb) $\pi^+\pi^-$ pairs. While the non-Coulomb background is assumed to have the same shape as the accidental background, the reconstruction of the Coulomb correlated background requires a modification

of the accidental background by the Coulomb correlation function [1]. The dependence of the Coulomb correlation function $A_C(Q)$ on the relative momentum Q, defined in the c.m.s. of the $\pi^+\pi^-$ pair, is well known from theory with high precision.

The procedure for getting the correct background shapes is hampered mainly by the following difficulties:

- multiple scattering in the target and in the detectors
- detector response for low-Q events
- different detector response for prompt and accidental events

Multiple scattering Simulations show that the $A_{2\pi}$ lifetime estimation is changed by 3.7% when the r.m.s. of the multiple scattering angle is changed by 1%. Experimentally multiple scattering is known with a precision of 1÷2% at energies of 100÷200 GeV (see Appendix A). In order to decrease the induced systematic errors in τ multiple scattering has to be measured for the Ni and Ti targets, in the detectors located upstream of the spectrometer magnet and in the aluminium membrane at the exit of the vacuum chamber. These measurements will be done by collecting a statistics of about 100 millions events to cover the total particle momentum range detected by the setup. For the Ni and Ti targets these measurements were started in 2002 and will be continued in 2003 during the data taking with the multi-layer target. We expected from these measurements a precision better than 1% (see Appendix A).

Detector response Part of the 2-track events detected have only one hit in the X or Y plane of the scintillation fiber detector (SFD) and double ionization in two planes of the ionization hodoscope of corresponding projection (IH). If two particles hit only one element of the SFD plane $X(Y)$ and produce double ionization in two $X(Y)$ planes of the IH, $Q_X(Q_Y)$ is measured correctly. But if two particles hit different elements $X(Y)$ and one of the hits is not detected, because of inefficiency of the SFD planes, the measurement of $Q_X(Q_Y)$ is wrong. The probability of such events depends on the SFD inefficiency to one particle detection ($\sim$5%), the response of the SFD electronics for two-particle detection by adjacent elements and the probability to mimic by a single particle the double ionization in the IH because of ionization-loss fluctuations. Given the measured SFD efficiency, its electronics response and amplitude characteristics of IH, we obtain corrections for the Q_X and Q_Y distributions which lead to change of the atomic pair number on $\sim$15%.

As this correction is clearly essential, it is necessary to measure directly the experimental distribution in $Q_X(Q_Y)$ of single hit events using a detector with a high efficiency and a better two-track resolution than the SFD. A new detector, Micro Drift Chambers, was developed and tested in 2002 which can be used for this purpose (see Appendix B). It has a two-hit resolution of $\sim 150\mu$m and an efficiency $\sim$100%. Its installation upstream of the SFD (fiber diameter of 500 μm) will allow to measure the one-hit distributions in $\Delta X(\Delta Y)$ and to compare them with their simulation.

Different detector response Correcting for the different responses of the SFD for accidental and prompt events introduces an uncertainty in the background determination, which can not be modelled with the necessary accuracy. However, the measurements with Micro Drift Chambers discussed in the prior paragraph will allow us to estimate experimentally both responses.

4 Study of systematic errors with the two target method

We propose to perform a measurement using a multi-layer target of total thickness equal to the standard single-layer target. In both cases we expect equal contributions from free Coulomb and non-Coulomb $\pi^+\pi^-$ pairs, and also equal shapes of the distributions. However, the multi-layer target will induce a flux of $\pi^+\pi^-$ pairs from $A_{2\pi}$ ionization ("atomic" pairs) which, compared to the single-layer target, will be about a factor two lower and will have a much weaker dependence on the $A_{2\pi}$ lifetime. For that reason after subtraction of the data collected with these two targets we will obtain the pure "atomic" pairs, and their amount will depend on the atom lifetime only. Moreover, uncertainties in calculation of the free pion pairs will contribute to the accuracy of this procedure in a significantly weaker way (about 4 times) than in the standard approach. Thus, the approach based on subtraction of data collected with the two target arrangements provides an alternative way to determine the $A_{2\pi}$ lifetime, which is less affected by systematic biases due to the uncertainty in the knowledge of the Coulomb pair yield. The details about the proposed measurement method are described in Appendices C and D. In a different combination, the same data may also be used to eliminate the signal and obtain the background alone. This would then provide a consistency check of our standard procedure for background reconstruction and a way to evaluate systematic errors arising from its estimation.

The collaboration has already started a series of measurements last September, using a multi-layer Ni target (12 foils, 8 μm thick, 96 μm total thickness). In order to really profit from this new two-target technique, a continuation of these measurements next year is essential. [1]

[1] Another way, already announced in a memorandum to the SPSC [2], to cross-check the reliability of the standard procedure which uses the Q-distribution of accidental pairs to reconstruct the background from free pairs, is to perform a measurement using a multi-layer Be target. With such arrangement the probability of atom break-up in the target is only a few percent (4% to compare to 43% in the standard Ni target). Therefore, the standard procedure should confirm the absence of detectable $A_{2\pi}$ in the low-Q region, if the spectrum of free pairs in the rest of phase space is correctly described. A detailed study on this method has been done in [3].

However beryllium and nickel have very different radiation lengths. This leads to a thickness of the Be target significantly larger than that of a Ni target (2 mm vs 100 μm) because one requires the same multiple scattering in the targets. Such a Be target has a much higher nuclear efficiency and would require a corresponding decrease of the beam intensity, but this cannot be provided by the PS. A measurement with a thinner Be target would require a large correction due to the difference in the multiple scattering and therefore cannot be used as a direct check of the Coulomb pairs distribution for the Ni target. Moreover Be and Ni have a ratio of Coulomb to non-Coulomb pairs different by 20% which again makes the distributions of free pion pairs not directly comparable.

5 Request in 2003

We would like to submit a request for beam-time in 2003 which allows DIRAC to complete the necessary systematics checks outlined above. We estimate that three months of running would provide sufficient statistics for the multi/single-layer target measurements. Moreover, we would like to propose a data taking plan which is compatible with other approved experiments (n-TOF) foreseen to run extensively next year.

The PS accelerator complex is able to provide simultaneous cycles to both DIRAC and the n-TOF facility. This, however, requires DIRAC to accept higher primary proton intensities, say above 1.2×10^{11} protons/spill on the target, 25% higher than at present. In this configuration, each machine cycle delivered to DIRAC would be followed by a parasitic cycle for n-TOF. This mode of PS operation would necessarily need a dedicated test, although both the PS/SPS coordinator and the PS machine experts have judged this to be feasible. To compensate the increase of primary proton intensity, we plan to use a Ni target thinner than the standard one, to reduce the interaction rate and restore the standard experimental conditions.

Our request for beam-time in 2003 is outlined as follows:

- The time between PS start (May 5th) and the beginning of n-TOF is estimated to be about 2 weeks, to complete beam setting for n-TOF. DIRAC would use that time at the standard intensity of 9×10^{10} protons/spill, and with 2 spills/supercycle, alternating single and multi-layer Ni targets, for normalisation purposes.

- The following 6 to 8 weeks at high intensity ($\geq 1.2 \times 10^{11}$), to run simultaneously with n-TOF, with 2.5$\div$3 spills/supercycle on average, using thinner (single and multi-layer) Ni targets. This amount of beam-time is calculated on the basis of the precision needed on systematics are compared to the overall statistical precision of DIRAC. This takes into account the similar amount of data collected by the end of 2002.

- After a 1 week technical stop to install a new detector, Micro Drift Chamber, we would like to request 2 weeks at high intensity, with 2 spills/supercycle, using thinner (single and multi-layer) Ni targets, and with a modified setup to measure the detection efficiency on closely-spaced tracks .

Appendices

A Multiple Scattering Measurements

The knowledge of the multiple scattering of pions in the target plays a crucial role in the DIRAC experiment. An essential part of systematic error in the experiment originates from uncertainties in the description of multiple scattering. The modern experimental status of the multiple scattering in a "thin" target is presented in Table 1.

Ref	**Beam**	**p, GeV/c**	**Target**	$x/X_0, \times 10^{-3}$	**Theory**	$\lvert\Delta\theta_{exp}\rvert, \%$
[4]	e^-	0.002	Al, Cu, Fe, Mo, Ag, Sn *Ta, Au, Pb*	$1.1 \div 2$	GS	$0 \div 1$ $10 \div 13$
[5]	e^-	0.157	Au *Be*	2.9, 5.8 *3.9, 7.5*	$M \times (Z+1)$	$1.2, 1.3$ $3.8, 5.3$
[6]	p^+	$0.001 \div 0.005$	Al, Ni, Ar, Au	$0.06 \div 1.4$	M	5
[7]	p^+	0.600	C, Al, Cu, Cd, Pb	$700 \div 2200$	$M_{c.m.}$	$3 \div 6$
[8]	$\pi^\pm$	$0.24 \div 0.33$	C, Al, Cu, Pb	$13 \div 150$	$M_{c.m.}$	$3 \div 6$
[9]	$\pi^\pm, K^\pm, p^\pm$	$50 \div 200$	H, Be, C, Al, Cu, Sn, Pb	$45 \div 70$	*M* *HF*	$1 \div 2$ $1 \div 10$
[10]	p^+	0.16	14 materials from Be to U and plastics	$0.1 \div 1000$	M_F *HF*	0.5 2.5

Table 1: *Review of multiple scattering measurements.* $|\Delta\theta_{exp}|$ *is the difference between theoretical and experimental values of multiple scattering angles.*
GS *Goudsmit – Saunderson multiple scattering theory [11];*
M *Molière multiple scattering theory [12];*
$(\boldsymbol{Z+1})$ *factor indicates that* $\boldsymbol{Z(Z+1)}$ *was used instead of* $\boldsymbol{Z^2}$ *is to take into account the scattering by the atomic electrons, as first suggested in [4];*
$\boldsymbol{M_{c.m.}}$ *Molière theory with center of mass correction. Later it was pointed out by [10] that this term is incorrect and thus the difference between predicted and measured angle should be slightly increased in [7, 8];*
HF *Highland formula [13] gives the scattering angle in terms of radiation length;*
$\boldsymbol{M_F}$ *Molière theory with Fano [14] corrections for incident particle scattering by atomic electrons as well as the screened Coulomb field of the nucleus.*

It is seen from the table that only a small number of experiments are useful for DIRAC and no one can be used directly, because our momentum range is not covered by any one. The analysis of the references gives us not better than 2% accuracy for the multiple scattering description.

Fortunately, the multiple scattering of pions in the target can be measured directly in the DIRAC setup [1]. For this measurement a foil, similar to the target, is placed between drift chambers in one arm of the DIRAC spectrometer just after the DC-3 chamber. The two parts

of track in DC, before and after the foil, are measured independently and they determine the multiple scattering angle. The sensitivity of the measurement is illustrated in fig. 2. The solid-line histogram is produced by real events, collected in fall 2002, and the dashed-line histogram is obtained by the same events when an additional multiple scattering angle is simulated according to the Highland's formulae [13]. The difference between the two histograms is seen very clearly. We hope to reach better than 1% accuracy in the description of multiple scattering in the target foil, because in parallel with the scattering events reference events will be collected. So, all experimental uncertainties cancel out.

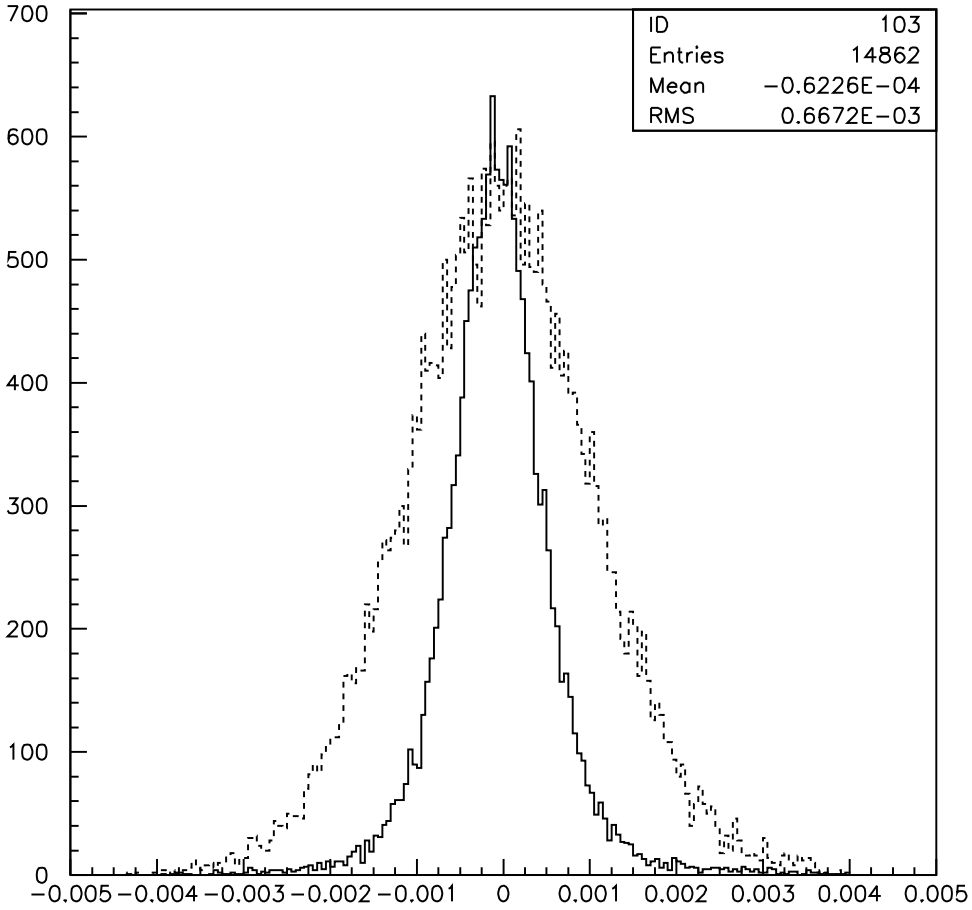

Figure 2: *Distribution of the angle between two parts of the pion track measured by the DIRAC drift chambers. Solid-line histogram — without additional multiple scattering; dashed-line — with simulation of additional multiple scattering in the nickel foil,* $94\ \mu m$ *thick. Pion momentum —* $1\ GeV/c$.

B Micro Drift Chambers as a DIRAC upstream coordinate detector

B.1 Introduction

The distinctive property of "atomic pairs" is the passage of two charged particles at a rather small relative distance when detected upstream of the magnet. Therefore, upstream coordinate detectors have to detect tracks with high spatial resolution and, at the same time, resolve nearby tracks. In the following we propose a design of Micro Drift Chamber (MDC), which combines high space and time characteristics with relatively high double track resolution.

Let us consider how particles are detected in a drift chamber cell. In the case of one particle, primary ionization electrons drift to an anode wire and initiate the avalanche process. This avalanche occupies part of the anode wire ("dead zone") and inhibits the detection of another particle close-by in space. An additional limitation arises from read-out electronics. Even if two particles were detected on the anode wire itself, a later signal might not be accepted by the multi-hit TDC due to the finite double-hit resolution. These limitations are fatal only in the case of a single-plane chamber. An additional plane, shifted by half a cell width, eliminates not only the left-right ambiguity, but also the double track resolution problem (fig. 3). If two tracks cross one cell, one particle is detected by the first plane and the other by the second plane.

In the same figure a schematic layout of a double plane chamber is presented. Each plane consists of 32 cells. The cell size is 3×2 mm^2, and the sensitive area is 94.5×94 mm^2.

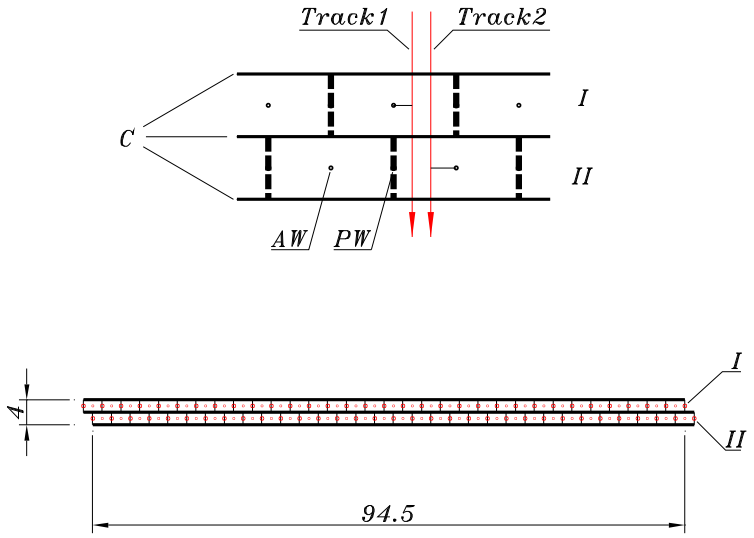

Figure 3: *Schematic layout of a double-plane drift chamber: AW — anode wires, 50 μm in diameter; PW — potential wires, 100 μm in diameter; C — cathode, Mylar foil, 20 μm thick. Sizes are measured in mm.*

The chamber will be operated in a high current avalanche mode with the gas mixture $\mathrm{Ar}/i\mathrm{C_4H_{10}}/\mathrm{H_2O}$. This will permit to use a drift chamber read-out electronics based on the present one which has demonstrated perfect operating features.

The drift parameters, time and space resolution of the chamber have been investigated with the help of the GARFIELD simulation package, and the counting rate capability has been estimated from our "dead zone" measurement. The gas mixture $\mathrm{Ar}(0.33) + i\mathrm{C_4H_{10}}(0.66) + \mathrm{H_2O}(0.01)$ was used in this simulation.

Drift times (T_{dr}) and spreads of arrival time (σ_t) as a function of drift distance are shown in fig. 4. The drift time T_{dr} exhibits a rather linear dependence, which is very convenient for track reconstruction procedures. The maximum drift time is 26 ns. The σ_t value never exceeds 0.5 ns, thus the spatial resolution is better than 30 μm.

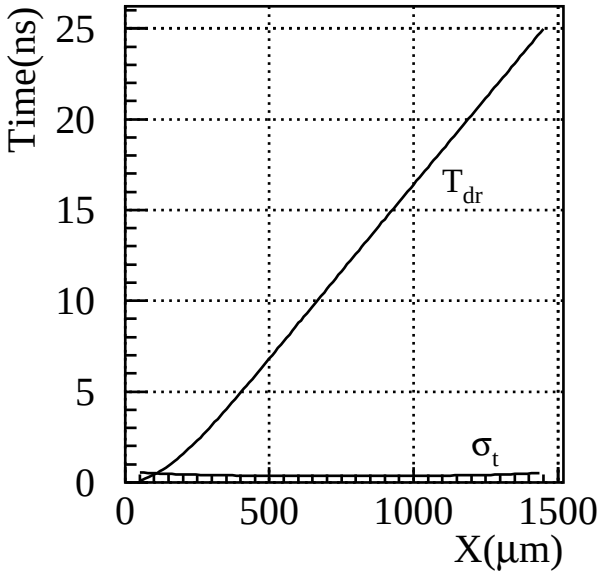

Figure 4: *Time features of the drift chamber simulated with help of the GARFIELD package. Gas mixture is* $\mathrm{Ar}(0.33) + i\mathrm{C_4H_{10}}(0.66) + \mathrm{H_2O}(0.01)$.

The double track resolution of the double-plane chamber is illustrated in fig. 5. The histograms correspond to two tracks separated by 100 μm in space. The left histogram corresponds to tracks detected by the first plane, and the right one to tracks detected by the second plane. The TDC bin width, of 0.5 ns, has been taken into account.

B.2 Present status of the Micro Drift Chamber project

We performed several software simulations and experimental measurements with few prototypes of micro drift chamber. These investigations permitted to design the micro drift coordinate detector, which consists of four double-plane chambers in each coordinate (X and Y), and one extra double-plane chamber with inclined wires to distinguish multi-hit events.

The design of the MDC was slightly changed in comparison with the first project. At present, the anode wire diameter is 20 μm, the anode wire pitch is 2.54 mm, potential wires are replaced by carbon coated Mylar strips, 20 μm thick, and the chamber sensitive size is now 80×80 mm^2.

The present drift chamber readout electronics is used for the MDC. Only the front-end electronic board was modified. The new one has ten times lower threshold, 10 μA instead of 100 μA for the old one.

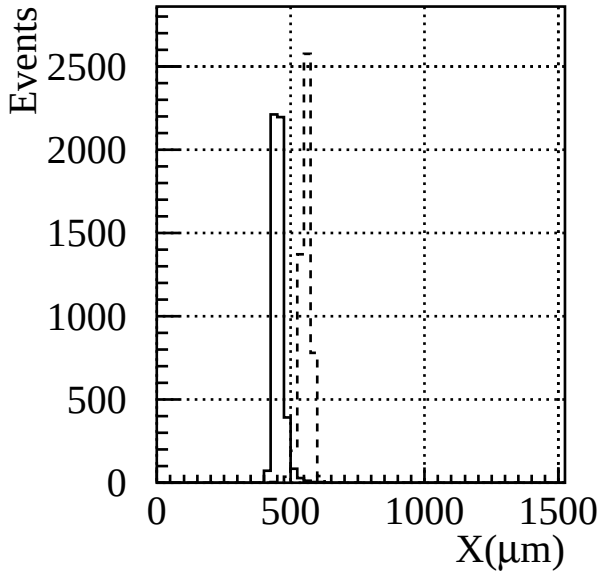

Figure 5: *The double track resolution of the double-plane drift chamber. The solid histogram corresponds to track position* 450 *μm and the dashed one to* 550 *μm with respect to the anode wire.*

The first MDC equipped by the new read-out electronics was extensively tested in real experimental condition. The counting rate capability of the detector was investigated at different threshold values. The chamber demonstrated excellent behaviour in rather hard radiation conditions. The width of the operational region in high voltage is more than $500\ V$ at the nominal threshold of 10 μA. Another kind of investigation was performed placing the MDC between present drift chambers of the DIRAC spectrometer to get information about drift properties and coordinate accuracy. A large amount of data was collected at different thresholds and high voltage values. This information will allow us to get complete knowledge about the MDC performance. The raw data collected in this test permit to get a first impression about the drift properties and coordinate accuracy. The time spectrum of the MDC signals is presented in fig. 6. The shape of the spectrum shows that the drift function is rather linear with a maximum drift time equal to about $23\ ns$. The right edge of the time spectrum provides an estimation of the coordinate accuracy $\sigma = 30\ ns$.

The most important features of the detector are:

- spatial accuracy $\sigma < 30$ μm,
- double track resolution < 200 μm,
- one plane efficiency at beam intensity $I = 2 \cdot 10^{11}$ protons per spill, due to the "dead zone" $> 98\%$,
- low multiple scattering: total detector thickness $< 5 \cdot 10^{-3}\ X_0$,
- time resolution $\sigma < 1$ ns,
- low track multiplicity < 3 tracks,

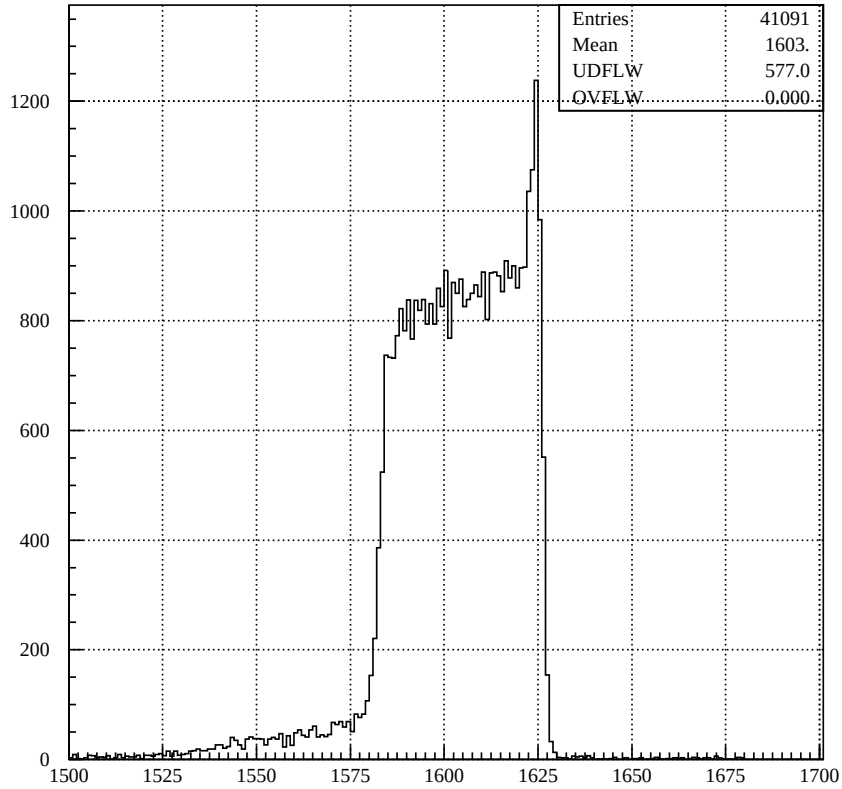

Figure 6: *Raw time spectrum of the micro drift chamber. Bin width - 0.5 ns. Gas mixture is* $\mathrm{Ar}(0.25) + i\mathrm{C_4H_{10}}(0.74) + \mathrm{H_2O}(0.01)$*, pressure -* $2\ atm$*.*

- small readout time < 3 μs.

The micro drift coordinate detector will be completely produced and tested before the 2003 run.

B.3 Micro drift chamber readout system

To readout events from micro drift chambers we will use a new version of the drift chamber readout system [15], which has been using in the experiment since 1999.

The only modification is a new time-to-digital converter (TDC) board. In this TDC board the threshold of the input discriminators was decreased from 100 μA to 10 μA and four fast OR outputs were provided for trigger purposes.

The on-chamber mounted TDC board (Fig.7), heart of the readout system, combines together the 16-channel amplifier/discriminator of input signals, the 16-channel TDC itself and a data buffer. The fast OR output is a logical OR of four discriminator outputs.

The discriminated hit wire signals are processed and selected in the 16-channel TDC. The hits found within a time window are buffered and then readout. The latest 16 hits, with respect to the STOP signal, in each channel of TDC can be recorded and processed. TDC operates in a common STOP mode therefore no additional delay in the recording channel is required.

During 2002 run this new TDC board was successfully tested on a particle beam.

To readout events from all micro drift chambers 40 TDC boards and 5 bus drivers (part of readout system) are needed. We plan to complete the production of all those devices by the beginning of May 2003.

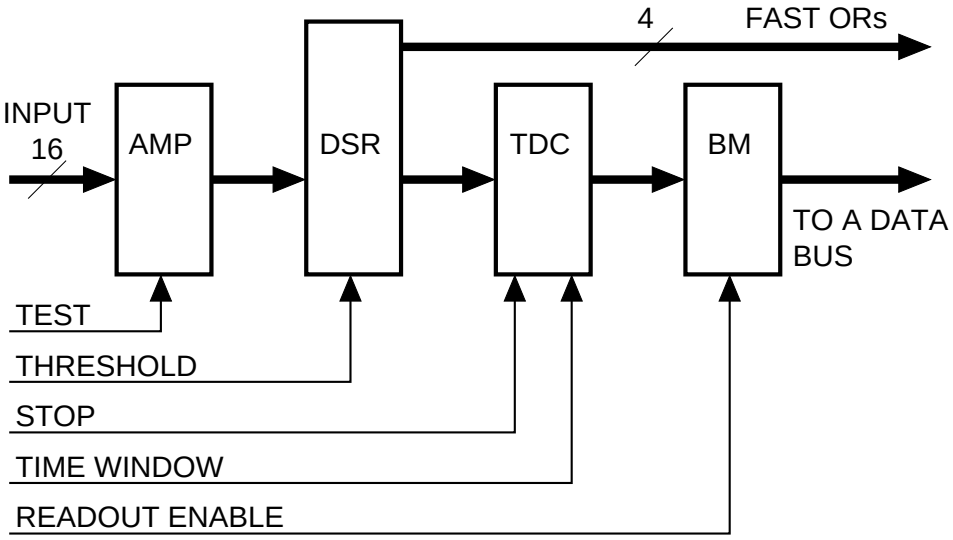

Figure 7: *Simplified block diagram of the TDC board. AMP — amplifier, DSR — discriminator, TDC – time-to-digital converter, BM – buffer memory.*

TDC board specification

Number of channels	16
Input impedance	150 Ω
Threshold range	10 – 1000 μA
Threshold tolerance (at threshold 10 μA)	$\pm 5\%$
Crosstalk	-41 db
Slewing (from 2 to 20 threshold)	1.6 ns
Fast OR outputs:	
number of outputs	4
signal levels differential	ECL
delay time	6 ns
maximum frequency	250 MHz
TDC:	
maximum number of hits in each channel	16
double pulse resolution	$<$10 ns
least count	0.5 ns
time measurement range	20 – 2048 ns
offset value	0 – 2048 ns
step of the range and offset setting	8 ns
time window width	16 – 2028 ns
differential non-linearity	$\pm$10%
Time of data processing and readout	$(\mathrm{N_r} + \mathrm{N_s} + 3) \cdot 100$ ns[2]
Power dissipation	6 Wt

C The two target method for the lifetime measurement

The method is based on measurements with two different target types: 1) Single-layer target and 2) Multi-layer target of same total thickness, but consisting of a few layers with 1 mm gaps in between. The main idea is to provide a "pure" experimental observation of $\pi^+\pi^-$ pairs from $A_{2\pi}$ break-up in the target. The difference between the observed distributions obtained with these two targets should only contain "atomic" pairs. The number of these "atomic" pairs depends on the atom lifetime τ. The method of lifetime extraction from these data is much less affected by the uncertainties in the procedure for selecting "atomic" and free pairs than in the standard method with a single-layer target only.

First let us consider the accuracy of our standard method. The number of real time-correlated events, in the range of small relative momentum for the standard, single-layer target is written:

$$N_R = N_{RA} - t \cdot N_{acc} = n_{A2\pi} + N_C + N_{nC} \ . \tag{1}$$

Here N_{RA} is the number of real and accidental events in the central time-peak; N_{acc} is the number of accidental events in their time windows; t is the ratio of the time windows of real and accidental events; $n_{A2\pi}$ is the number of observed atomic pairs; N_C and N_{nC} are the numbers of the "Coulomb" and "non-Coulomb" pairs, respectively.

The probability of $A_{2\pi}$ break-up, which is the ratio between the total number of the broken atoms $n^{\rm tot}_{A2\pi}$ and the total number of produced ones $N^{\rm tot}_{A2\pi}$, can be expressed via the number of atomic pairs in the selected range of the small relative momentum $n_{A2\pi}$ and the number of "Coulomb" and "nonCoulomb" pairs in the same range, N_C and N_{nC}:

$$P_{\rm br} = \frac{n^{\rm tot}_{A2\pi}}{N^{\rm tot}_{A2\pi}} = \frac{m \cdot n_{A2\pi}}{k' \cdot N_C} = \frac{n_{A2\pi}}{k \cdot N_C} = \frac{N_R - N_{Cf} - N_{nCf}}{k \cdot N_{Cf}} \ . \tag{2}$$

Here the index f indicates the results obtained from the standard fitting procedure. The coefficients m, k' and k are obtained from a Monte-Carlo simulation of the processes of atoms break-up and detection of pions pairs. In further calculations the value $k = 0.54$ for the range of relative momentum $F < 2$ has been used. ($F = \sqrt{(Q_x/\sigma_x)^2 + (Q_y/\sigma_y)^2 + (Q_z/\sigma_z)^2}$, $Q_{x(y,z)}$ and $\sigma_{x(y,z)}$ are the components and corresponding resolutions of the pair c.m.s. relative momentum.)

The variance of the estimated number of atomic pair is written:

$$\begin{aligned} \sigma^2_{n_{A2\pi}} \ &= \ \sigma^2_{N_R} + \sigma^2_{N_{Cf}} + \sigma^2_{N_{nCf}} + 2 \cdot cov(N_{nCf}, N_{Cf}) + \\ &\quad 2 \cdot t \cdot cov(N_{Cf}, N_{acc}) + 2 \cdot t \cdot cov(N_{nCf}, N_{acc}) \ . \end{aligned} \tag{3}$$

Then the variance of the break-up probability is expressed as:

$$\sigma^2_{P_{\rm br}} = P^2_{\rm br} \cdot \left[\frac{\sigma^2_{n_{A2\pi}}}{n^2_{A2\pi}} + \frac{\sigma^2_{N_{Cf}}}{N^2_{Cf}} + 2 \cdot \frac{\sigma^2_{N_{Cf}} + cov(N_{nCf}, N_{Cf}) + t \cdot cov(N_{Cf}, N_{acc})}{n_{A2\pi} \cdot N_{Cf}} \right] \ . \tag{4}$$

For the second target, consisting of a few layers with 1 mm gaps and with the same total thickness, the number of events in the same range of small relative momentum (assuming the same number of primary interactions) is written as:

$$N2_R = N2_{RA} - t \cdot N_{acc} = n2_{A2\pi} + N_C + N_{nC} \ . \tag{5}$$

The number of atomic pairs $n2_{A2\pi}$ for this target is smaller and its dependence on the lifetime is much weaker than with the standard target (see Fig.8). Thus the following combination depends on the $A_{2\pi}$ lifetime in a unique way

$$V(\tau) = \frac{N_R - N2_R}{N_{Cf}} = \frac{n_{A2\pi} - n2_{A2\pi}}{N_{A2\pi}/k} = \frac{N_{A2\pi}(P_{\rm br1} - P_{\rm br2}) \cdot k}{N_{A2\pi}} = (P_{\rm br1}(\tau) - P_{\rm br2}(\tau)) \cdot k \ . \tag{6}$$

Here $P_{\rm br1}$ and $P_{\rm br2}$ are the calculated probabilities of atom break-up for each target and k comes from the relation $N_{A2\pi} = kN_C$ (see Eq.2). Then the variance of V is written as:

$$\sigma_V^2 = V^2 \cdot \left[\frac{\sigma_{N_R}^2 + \sigma_{N2_R}^2}{(N_R - N2_R)^2} + \frac{\sigma_{N_{Cf}}^2}{N_{Cf}^2} + 2 \cdot t \cdot \frac{cov(N_{Cf}, N_{acc})}{(N_R - N2_R) \cdot N_{Cf}} \right] \ . \tag{7}$$

A detailed comparison of Eq.4 and Eq.7 shows that the contributions of N_{Cf}^2 and $\sigma_{N_{Cf}}^2$, which have the largest systematic uncertainties, are significantly smaller for V than for $P_{\rm br}$. Thus, the measurements of $P_{\rm br}$ and V allow us to obtain the lifetime in the two different approaches and get an estimation of the probable systematic bias.

To get a numerical estimation of the required statistics, the data collected in 2001 with the Nickel target have been used: $N_R = 17696 \pm 135$, $N_{Cf} = 13763 \pm 250$ and $n_{A2\pi} = 3265 \pm 259$.

The first column of Table 2 contains information for the standard fitting procedure, all other for the two-target method with different numbers of layers in the second target. The meanings of the rows labels are: "Layers" is the number of layers in the target; "Thickness" is the thickness of one layer in μm; "$P_{\rm br}$" is the calculated probabilities of the atom break-up in each target, V is the variable defined in Eq.6; "Derivative" is $dP_{\rm br1}/d\tau$ for the first column and $dV/d\tau$ for all other; $\delta_{10\%}$ and $\sigma_{10\%}$ are the relative and absolute accuracy, respectively, of the measured value ($P_{\rm br}$ or V) which provides the 10% accuracy in the lifetime measurement; $\sigma_{\rm stat}$ is the accuracy in the measured values ($P_{\rm br1}$ or V) achieved (or could be achieved) with the Nickel 2001 data. For the case of the two-target method, the data were divided into equal parts.

Table 2:

Layers	1	5	10	20
Thickness (μm)	100.	20.0	10.	5.
$P_{\rm br}$	0.44704	0.33396	0.25373	0.17803
V		$6.106 \cdot 10^{-2}$	0.10439	0.14526
Derivative	$5.654 \cdot 10^{-2}$	$1.817 \cdot 10^{-2}$	$2.511 \cdot 10^{-2}$	$2.832 \cdot 10^{-2}$
$\delta_{10\%}$	$3.667 \cdot 10^{-2}$	$8.631 \cdot 10^{-2}$	$6.976 \cdot 10^{-2}$	$5.655 \cdot 10^{-2}$
$\sigma_{10\%}$	$1.640 \cdot 10^{-2}$	$5.270 \cdot 10^{-3}$	$7.282 \cdot 10^{-3}$	$8.214 \cdot 10^{-3}$
$\sigma_{\rm stat}$	$4.167 \cdot 10^{-2}$	$1.942 \cdot 10^{-2}$	$1.927 \cdot 10^{-2}$	$1.911 \cdot 10^{-2}$

The required improvement in the statistical accuracy with respect to the Nickel 2001 data is almost the same for the single target measurement and the two-target measurement for the case of 10 layers. Thus the two-target method with a number of layers in the second target between 10 and 20 looks like a very attractive addition to our standard procedure of the lifetime measurement.

The behaviours of the dependence of $P_{\rm br}$ and V on the lifetime τ which have been employed for to get values for Table 2 are shown in Figs.8 and 9.

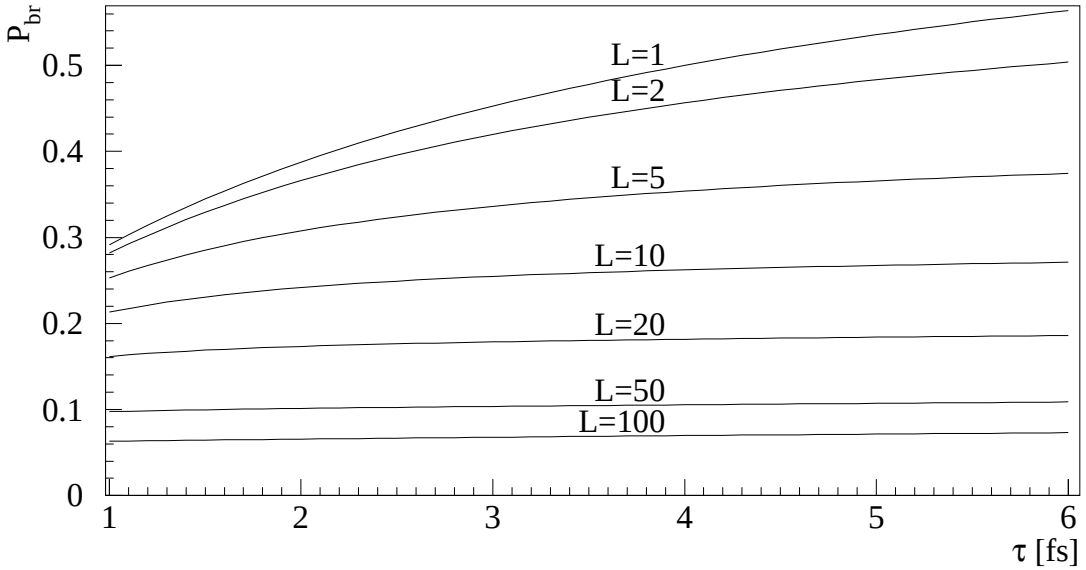

Figure 8: *The probability of $A_{2\pi}$ break-up in the Nickel targets consisting of the different number of layers (L) with 1 mm gap between and having a total thickness of 100 μm as a function of the lifetime τ.*

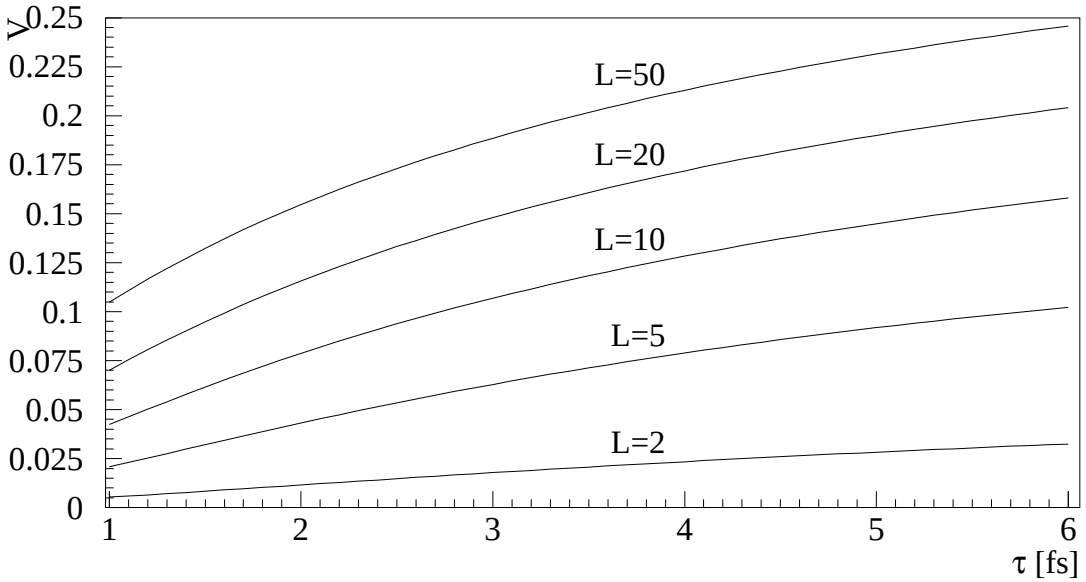

Figure 9: *Variable V defined in Eq.6 as a function of the $A_{2\pi}$ lifetime τ for different number of layers (L).*

D Features on the Nickel multi-layer target

D.1 Introduction

DIRAC collaboration has recently installed a new multi-layer Nickel target. This setup was designed as an alternative to the single-layer target measurement with two goals in mind: first, to provide a cross-check of very low relative momentum atomic and pion pair reconstruction and, second, to obtain an independent measurement of pionium lifetime.

Two main design requirements had to be fulfilled:

- Its total thickness had to be the same as the main single-layer target in order to reproduce the same multiple scattering effects on the low relative momentum spectrum of pion pairs.
- The break-up probability of a multi-layer target is reduced when compared to the single-layer setup since the atomic pairs found in the interstitial vacuum gaps have no possibility of being broken up and, hence, they annihilate. Taking into account physical and economic constraints we optimized the thickness of the individual layers to minimize break-up probability of pionium for this setup.

The final design consisted of an array of 12 layers just under than 8 μm each, separated by gaps of 1 mm. The final measured thicknesses per layer are shown in Table 3 [3].

Under the standard experimental conditions of DIRAC the multi-layer target was found to yield the value of $P_{br} = 0.2314 \pm 0.0005$ for the break-up probability, which should be compared with $P_{br} = 0.4696$ values for the single 98μm target.

Below we examine the possible sources of systematical effects, such as the irregularities on the Nickel layer surface, the influence of the difference in the total thickness of the single and multi-layer targets either in the breakup probability result or in the multiple scattering of pairs.

Layer	1	2	3	4	5	6	7	8	9	10	11	12
(μm)	7.94	7.94	7.98	7.94	7.98	7.96	7.97	7.97	7.96	7.99	8.00	8.00

Table 3: Individual layer thicknesses for the multi-layer target.

D.2 Break-up probability and thickness

D.2.1 Break-up probability and fluctuations in thickness

We have studied the effect of possible irregularities of the layer surface which could alter the total amount of matter that a pionic atom would traverse in the multi-layer target (see Figure 10). The irregularities can be modeled by randomly varying the thickness of every layer of the target. The fluctuations in thickness are sampled from uniform distributions centered around the average measured thicknesses for each layer. Several distributions widths have been used for this study.

[3] These results have been obtained by weight measurements. Recently the layers thicknesses have been measured with X-rays achieving compatible values. Moreover, the total thickness difference with the single layer can be precisely determined by measuring counting rates in DIRAC setup.

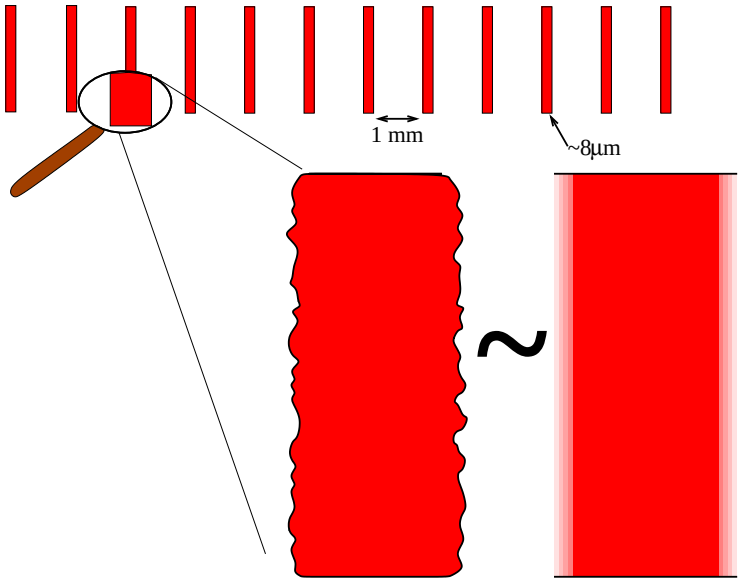

Figure 10: Irregular layer surface can be modeled as randomly varying thickness.

Assuming fluctuations in the target thickness of up to $0.8\mu m$ for each layer (which represents more than 10% their total thickness) the value of the break-up probability is $P_{br} = 0.2317 \pm 0.0005$. Increasing the maximum value of the fluctuations to 1.6μm (more than 20%) around the mean, the result is found to be $P_{br} = 0.2311 \pm 0.0005$. If we compare both results with the mean of $P_{br} = 0.2314 \pm 0.0005$ we conclude that the effect of thickness fluctuations turns out to be negligible.

D.2.2 Break-up probability and systematical biases in the total thicknesses of the layers

We have also considered the effect of systematic change in thickness of every layer leading to a change in the total thickness [4]. We have calculated the break-up probability assuming the thickness of every single-layer to be 0.8 μm larger than the measured result ($\sim 10\%$ larger). In this case the breakup probability yields $P_{br} = 0.2438 \pm 0.0005$, or around 5% larger than the nominal value.

Also, decreasing the thicknesses of the target layers by 0.8 μm we get $P_{br} = 0.2190 \pm 0.0005$, around 5% less than in the original case.

However, these two cases are extreme since we can establish the total thickness difference between the multi and single-layer targets with a precision better than 1%, by measuring the counting rates in DIRAC setup, leading to an uncertainty in the break-up of less than 0.5%.

D.3 Multiple scattering

Since in our experiment we are interested primarily in the very low relative momentum region of the pion pair spectrum, it is crucial to evaluate the effect of multiple scattering. Hence, the multi-layer target was designed to have the same total thickness as the single layer targets we have been mainly using during 2000, 2001 and 2002 data taking runs. 100% accuracy,

[4] This type of bias could be produced by a systematic error in the thickness measurements.

however, can be never achieved due to inaccuracy in the manufacturing process, which is also the case for DIRAC. For the requested Ni target thickness of 100μm, we were supplied with 94μm thick target (used until July 2001), and the second Ni target used currently is 98μm. The overall multi-layer target thickness, at requested 95μm, is in fact 95.63μm.

To test the influence of the thickness differences we have made a Monte Carlo check comparing the spectra of Coulomb background pairs for three cases of the two single and the multi-layer targets. The result, seen in Figure 11, shows slight variations between the three cases. However, this variation is not larger than 0.5% in the region where $Q < 3$ MeV/c where the atomic pairs can be found.

This analysis has been performed only at the generation level by computing the multiple scattering effect in the targets with a relatively simple routine. We have also made a more detailed analysis using the GEANT-DIRAC program, which performs a full simulation of the spectrometer behavior, and reconstructed the resulting events with the standard DIRAC analysis procedure. This study accounts not only for the multiple scattering effects but also for the tracking resolution and the different geometries of the target systems. The result of this analysis with Coulomb pairs can be seen (for the 98μm target and the multi-layer target cases) in Figure 12. We can conclude that, even though we can observe a slight systematical bias leading to a small enhancement of the $12 \times 8\mu$m sample, the discrepancy is much smaller than the statistical error after approximately two months of DIRAC data taking. Moreover, the difference is of the order of 2 percent for $Q < 3$ MeV/c.

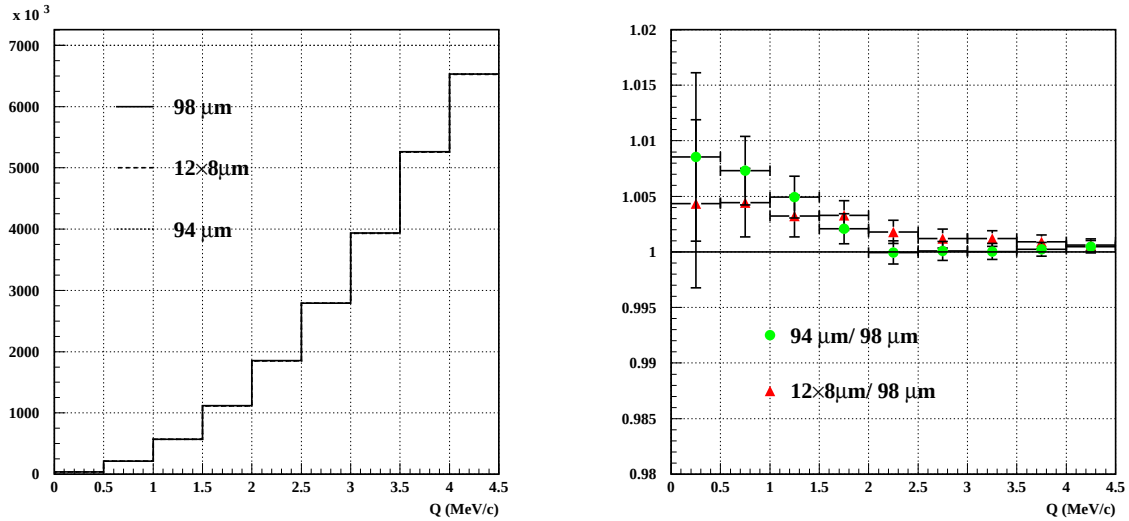

Figure 11: **On the left**, integrated spectrum of Coulomb pairs after the target at the Monte Carlo generation level. Spectra for three targets (98 and 94 μm single targets and $12 \times 8\mu$m multi target) are shown (they cannot be distinguished). **On the right**, integrated ratio between the spectra taking the spectrum from the 98μm target as a reference.

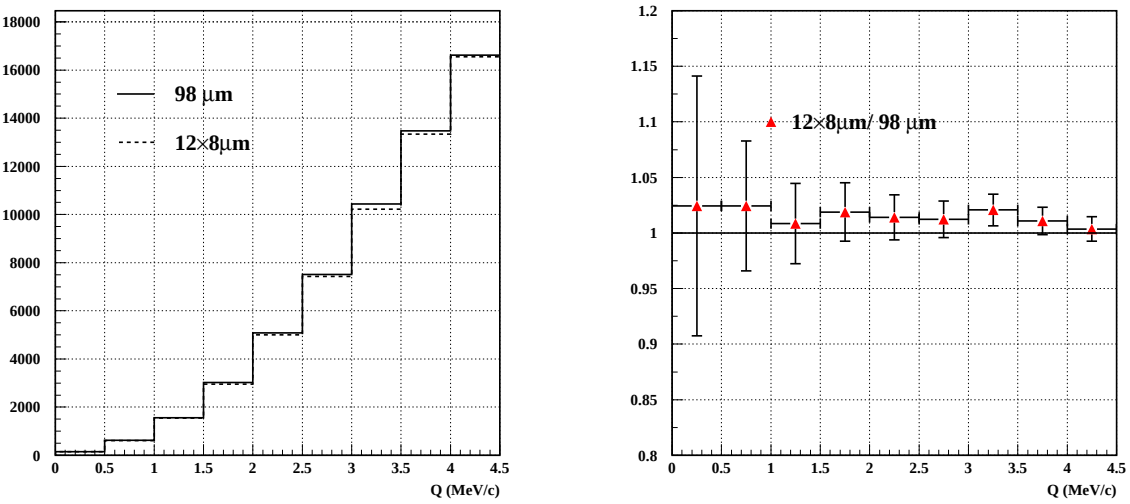

Figure 12: **On the left**, integrated spectrum of Coulomb pairs after the target after full GEANT simulation and standard DIRAC reconstruction. Only two target (98 μm single target and $12 \times 8\mu$m multi target) spectra are shown. **On the right**, integrated ratio between the spectra.

References

[1] B. Adeva et al., *Proposal to the SPSLC: Lifetime measurement of $\pi^+\pi^-$ atoms to test low energy QCD predictions*, CERN/SPSLC/P 284 (1994).

[2] Memorandum (DIRAC Collaboration) (CERN/SPSC 2002-018, SPSC/M-684, May 14 2002).

[3] C. Santamarina Rios, L. Tauscher *A proposal to measure Coulomb background with a multilayer Beryllium target*, DIRAC NOTE 02-07.

[4] L.A.Kulchitscky, G.D. Latyshev, Phys.Rev.**61**(1942) p.254.

[5] A.O.Hanson et al., Phys.Rev. **84**(1951) p.634.

[6] H.Bichsel, Phys.Rev. **112**(1958) p.182.

[7] E.V.Hungerford et al., Nucl.Phys. **A197**(1972) p.515.

[8] B.W.Mayes et al., Nucl.Phys. **A230**(1974) p.515.

[9] G.Shen et al., Phys.Rev.D**20**(1979) p.1584.

[10] B.Gottschalk et al., Nucl.Instr. and Meth. B**74**(1993) p.467.

[11] S.Goudsmit and J.L.Saunderson, Phys.Rev. **58**(1940) p.37.

[12] G.Moliére, Z.Nuturforsch. **3a**(1948) p.78.

[13] V.L.Highland, Nucl.Instr. and Meth. **129**(1975) p.497.

[14] U.Fano, Phys.Rev. **93**(1954) p.117.

[15] L.Afanasyev and V.Karpukhin, NIM A 492 (2002) 351-355; arXiv:hep-ex/0208011.